Nanoparticles

International Edition: DOI: 10.1002/anie.201602795
German Edition: DOI: 10.1002/ange.201602795

Luminescent Gold Nanoparticles with Size-Independent Emission

*Jinbin Liu[+], Paul N. Duchesne[+], Mengxiao Yu[+], Xingya Jiang, Xuhui Ning, Rodrigo D. Vinluan III, Peng Zhang, and Jie Zheng**

Abstract: *Size-independent emission has been widely observed for ultrasmall thiolated gold nanoparticles (AuNPs) but our understanding of the photoluminescence mechanisms of noble metals on the nanoscale has remained limited. Herein, we report how the emission wavelength of a AuNP and the local binding geometry of a thiolate ligand (glutathione) on the AuNP are correlated, as these AuNPs emit at different wavelengths in spite of their identical size (ca. 2.5 nm). By using circular dichroism, X-ray absorption, and fluorescence spectroscopy, we found that a high Au–S coordination number (CN) and a high surface coverage resulted in strong Au^{I}–ligand charge transfer, a chiral conformation, and 600 nm emission, whereas a low Au–S CN and a low surface coverage led to weak charge transfer, an achiral conformation, and 810 nm emission. These two size-independent emissions can be integrated into one single 2.5 nm AuNP by fine-tuning of the surface coverage; a ratiometric pH response was then observed owing to strong energy transfer between two emission centers, opening up new possibilities for the design of ultrasmall ratiometric pH nanoindicators.*

Whereas size-dependent emission as a characteristic phenomenon of noble metals on the nanoscale has been well understood in the past decade,[1] size-independent emission is also widely observed for noble-metal nanoparticles (NPs)[2] and has found broad applications in cancer detection,[3] kidney functional imaging,[4] and chemical sensing.[5] For instance, strong size-dependent luminescence has been observed for Au nanoclusters (NCs) encapsulated by amine-terminated dendrimers: following a free-electron model, their emission maxima were shifted from the UV to the IR range with a size increase from Au_5 to Au_{31}.[1a] In contrast, AuNPs with the same size (ca. 2–3 nm) but coated with the thiolate ligand glutathione (GSH) can emit different colors with either $\lambda = 600$ nm[6] or 810 nm.[3a,7] Aside from these few-nanometer-large GSH-coated AuNPs (GS-AuNPs), differently sized few-atom GSH-protected AuNCs ($Au_{29}SG_{27}$, $Au_{30}SG_{28}$, $Au_{36}SG_{32}$, $Au_{39}SG_{35}$, $Au_{43}SG_{37}$) can exhibit the same emission peak at $\lambda = 610$ nm.[8] Wang and co-workers reported a series of thiolated AuNCs (Au_{11}, Au_{38}, Au_{140}, Au_{201}) with NIR luminescence from 800 to 1300 nm,[2a] similar to the NIR emission found for approximately 1.8 nm AuNPs.[9] Moreover, these phenomena are not limited to GS-AuNPs; AuNPs coated with other thiolate ligands also emit different colors even when their sizes are comparable. For example, 6-mercapto-1-hexanol-capped AuNPs can fluoresce at different wavelengths from 510 to 600 nm while the particle size hardly changes and remains to be within 2–3 nm.[10] These results clearly indicate that particle size is not a critical factor in determining the emission wavelengths of ultrasmall thiolated AuNPs. However, the origin of size-independent emission remains to be a mystery and limits our understanding of the photoluminescence of noble-metal NPs.

Herein, we revisited the structure–emission relationships of GS-AuNPs emitting at 600 and 810 nm with identical sizes of 2.5 nm. By using circular dichroism (CD) spectroscopy and elemental analysis, we found a significant difference between these two types of GS-AuNPs: the high GSH surface coverage on the 600 nm-emitting NPs resulted in an ordered and chiral conformation, whereas the low GSH surface coverage on the 800 nm-emitting NPs led to little chirality. As further revealed by X-ray absorption spectroscopy, the 600 nm-emitting GS-AuNPs had a higher degree of Au–S bonding than the 810 nm-emitting GS-AuNPs, indicating that the distinct Au local bonding environments are responsible for 600 and 800 nm emission (Figure 1 A). As the different emission wavelengths were independent of the AuNP size but depended on the surface coverage and local bonding environment, we were able to achieve 600 nm and 810 nm emission with one single AuNP by simply tuning the GSH surface coverage. Interestingly, the dual-emissive AuNPs exhibited unique ratiometric pH-dependent emissions, which were found to be due to strong energy transfer between two emission centers on the same particle.

GS-AuNPs with 600 nm or 810 nm emission were synthesized by controlling the GSH/$HAuCl_4$ ratio during reduction of $HAuCl_4$ in the presence of L-GSH at 95 °C (see the Supporting Information).[3a,7a] Using a GSH/$HAuCl_4$ ratio of 1.6:1, we synthesized luminescent AuNPs with a single emission peak at $\lambda = 600$ nm (quantum yield = 5.3 %, using Nile Blue A as the standard; Figure 1 B). When the GSH/$HAuCl_4$ ratio was decreased to 0.8:1, the $\lambda = 600$ nm emission disappeared, and we obtained AuNPs with a single emission peak at $\lambda = 810$ nm (quantum yield = 1.1 %, using Nile Blue A as the standard; Figure 1 C). The excitation spectrum also changed: the excitation maximum of the 600 nm-emitting GS-

[*] Dr. J. B. Liu,[+] Dr. M. X. Yu,[+] X. Y. Jiang, X. H. Ning, R. D. Vinluan III, Prof. Dr. J. Zheng
Department of Chemistry and Biochemistry
The University of Texas at Dallas
800 W. Campbell Rd., Richardson, TX 75080 (USA)
E-mail: jiezheng@utdallas.edu
Prof. Dr. J. Zheng
Department of Urology
The University of Texas Southwestern Medical Center
5323 Harry Hines Blvd., Dallas, TX 75390 (USA)
P. N. Duchesne,[+] Prof. Dr. P. Zhang
Department of Chemistry, Dalhousie University
6274 Coburg Rd., Halifax, NS, B3H 4J3 (Canada)
[+] These authors contributed equally to this work.

Supporting information for this article can be found under: http://dx.doi.org/10.1002/anie.201602795.

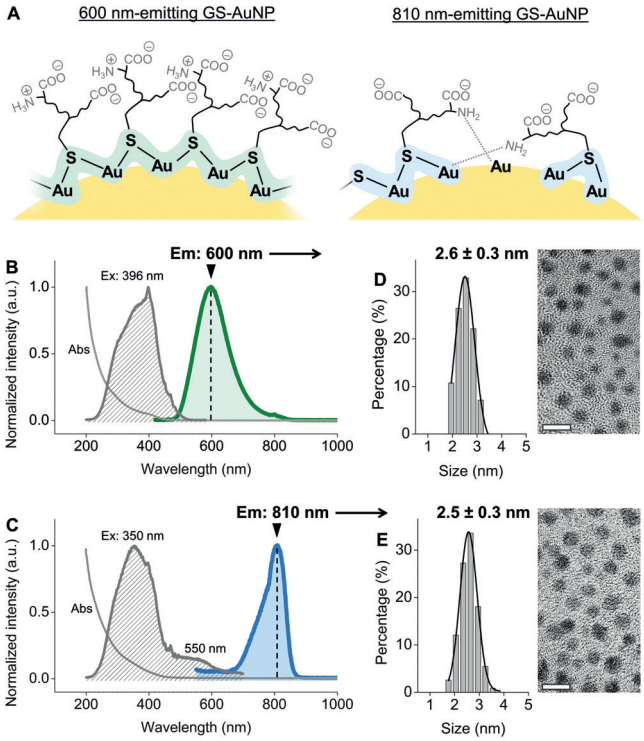

Figure 1. A) The two different local Au bonding environments of GS-AuNPs that correspond to 600 and 810 nm emission. Two amide bonds of glutathione are omitted for clarity. B, C) Absorption, excitation, and emission spectra of the 600 nm-emitting (B) and 810 nm-emitting (C) GS-AuNPs. D, E) TEM images and core-size distributions of the 600 nm-emitting (D) and 810 nm-emitting (E) GS-AuNPs. Scale bars: 5 nm.

AuNPs was located at $\lambda = 396$ nm, whereas that of the 810 nm-emitting GS-AuNPs was located at $\lambda = 350$ nm with a shoulder peak at $\lambda = 550$ nm (Figure 1 B, C). Despite these distinct excitation and emission spectra, the 600 nm- and 810 nm-emitting AuNPs had almost identical core sizes (2.6 ± 0.3 nm vs. 2.5 ± 0.3 nm; Figure 1 D, E). The absorption spectra of these two AuNPs were also very similar and showed strong absorption in the UV region, as well as a shoulder peak at approximately $\lambda = 400$ nm (Figure 1 B, C). IR spectroscopy confirmed that the two types of AuNPs had the same ligand, GSH. Characteristic peaks of GSH were observed, including the $\nu_s(COO^-)$ band at about $\lambda = 1390\ cm^{-1}$, the $\nu_{as}(COO^-)$ band at approximately $1595\ cm^{-1}$, and amide II at $1523\ cm^{-1}$ while the S–H stretching mode usually observed at about $2522\ cm^{-1}$ disappeared owing to the formation of Au–S bonds (see the Supporting Information, Figure S1).

The large Stokes shifts (> 200 nm; Figure 1 B, C) and microsecond lifetimes[6a] recorded for these GS-AuNPs suggested that the emission involves charge transfer between a Au center and a surface ligand ($Au^I \rightarrow S$)[1c] rather than a Au–N interaction.[1a] Therefore, we first studied the ligand conformation by CD spectroscopy. The 600 nm-emitting GS-AuNPs gave a negative band at 354 nm and a positive band at 400 nm (Figure 2 A), suggesting a highly ordered and chiral conformation for GSH on the AuNPs, which is consistent with previous reports on GSH-protected AuNCs[11] and other thiolated AuNPs.[12] As L-GSH has a weak CD response above 250 nm,[11a] the observation of such CD signals in the range of 300–500 nm implies the chiral arrangement of monomeric RS–Au–SR or dimeric RS–Au–SR–Au–SR staple motifs.[12c,d,13] Like free L-GSH, the 810 nm-emitting GS-AuNPs did not give a significant peak at 300–500 nm, indicating the random arrangement of GSH on the Au surface.

The two types of GS-AuNPs also have dramatically different Au bonding environments, which was revealed by extended X-ray absorption fine structure (EXAFS) spectroscopy, a technique that has been intensively used to study Au thiolate NCs.[14] For the 810 nm-emitting GS-AuNPs, the average coordination number (CN) of Au–S was determined to be 1.4 (Figure 2 B and Table S1). In the case of the 600 nm-emitting GS-AuNPs, the Au–S CN increased to 1.8 (Figure 2 C and Table S1). Aside from the approximately 29% increase in the Au–S CN (1.4 vs. 1.8), the Au–N CN decreased by about 44% (0.9 vs. 0.5) once the emission had been shifted from 800 nm to 600 nm, further suggesting two distinctly different local bonding environments.

These differences in ligand conformation and local bonding environment originate from the different GSH surface coverage on the AuNPs. Consistent with the higher GSH/$HAuCl_4$ ratio used for making the 600 nm-emitting AuNPs, the GSH surface coverage on the 600 nm-emitting AuNPs was nearly two times higher than on the 810 nm-emitting AuNPs (determined by elemental analysis, see the Supporting Information). The high GSH surface coverage on the 600 nm-emitting NPs can also be correlated with the large

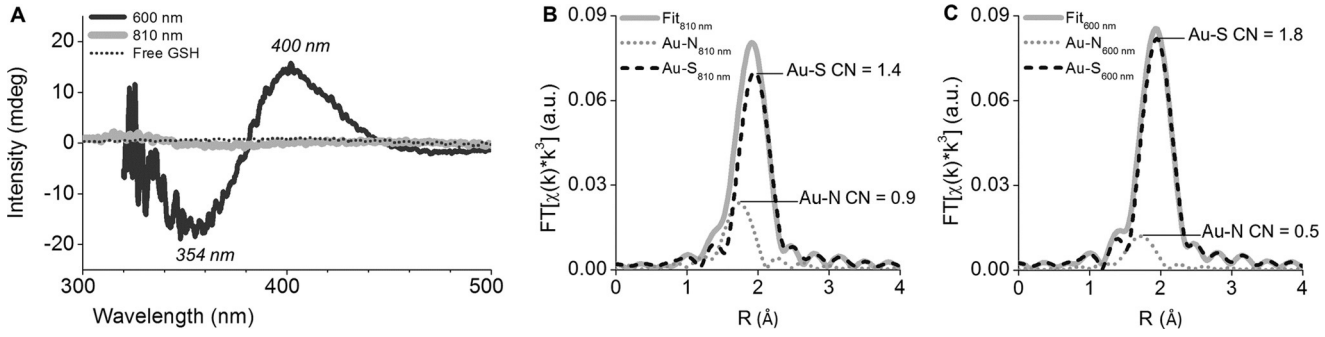

Figure 2. A) CD spectra of the 810 nm- and 600 nm-emitting GS-AuNPs. Data for free L-GSH shown for comparison. B, C) EXAFS spectra of the 810 nm-emitting (B) and 600 nm-emitting (C) GS-AuNPs at pH 7.0. CN = coordination number.

Au–S CN of these NPs (1.8), where densely packed GSH gives a chiral conformation. On the other hand, owing to the relatively low GSH surface coverage on the 810 nm-emitting AuNPs, there were not enough S atoms to stabilize the NPs; therefore, N atoms start interacting with Au, leading to an increase in the Au–N CN; this interaction, however, is not involved in the luminescence.[1a] As a result, the distinct surface coverage of GSH results in two types of emission centers: a higher degree of Au–S bonding resulted in strong Au→S charge transfer and served as the "600 nm emission center", whereas a lower degree of Au–S bonding led to relatively weak Au→S charge transfer and formed the "810 nm emission center" (Figure 1A).

Inspired by the finding that the size-independent emissions from GS-AuNPs were governed by the surface coverage, we controlled the surface coverage by tuning the GSH/$HAuCl_4$ ratio and were able to synthesize AuNPs with dual emission at $\lambda = 600$ and 810 nm (see the Supporting Information). The dual-emissive AuNPs had a core size identical to those of the single-emissive GS-AuNPs (2.5 ± 0.3 nm; Figure 3A). IR spectroscopy confirmed that the ligand was GSH (Figure S2). The GSH surface coverage on the dual-emissive NPs was 55% less than on the 600 nm-emitting GS-AuNPs but 14% higher than on the 810 nm-emitting GS-AuNPs (see the Supporting Information). The CD spectrum showed a positive peak at 348 nm and two negative peaks at 290 and 408 nm (Figure 3B), implying the presence of Au–S motifs with different conformation on the AuNPs.

The integration of the 600 nm and 810 nm emission centers in one single NP resulted in a synergistic effect: the dual-emissive GS-AuNPs can respond to pH changes in a ratiometric way. As the pH value increased from 5.0 to 9.0, the intensity of the 600 nm emission increased by a factor of four while the 810 nm emission intensity decreased by a factor of two, giving an isosbestic point at 730 nm (Figure 3C). Neither of the two single-emissive GS-AuNPs, nor a mixture of them, possesses this property. Single 810 nm emission was insensitive to pH changes, whereas single 600 nm emission only increased by a factor of 1.8 when the pH changed from 5.0 to 9.0 (Figures S3 and S4). The two single-emissive GS-AuNPs independently responded to pH changes in a mixture, generating a 2.4-fold intensity increase for emission at 600 nm and a negligible intensity change at 810 nm (no isosbestic point was detected; Figure S5). These differences confirm that the dual emissions with ratiometric pH response indeed originate from a single particle containing two coupled emission centers. Furthermore, the pH value of the solution can be determined by measuring the ratio of the intensities of the 810 nm and 600 nm emissions (I_{810}/I_{600}). The I_{810}/I_{600} value increased by a factor of almost four within the physiological pH range from 7.4 to 5.0. The pH threshold for the observed pH-dependent emission was pH 6.65 (Figure 3D). The reversible pH response suggested that the GS-AuNPs are very stable over this pH range (Figure 3E). The emission spectra of the dual-emissive GS-AuNPs were also independent of the ionic strength of the solution (Figure S6).

The ratiometric response of the dual-emissive GS-AuNPs was attributed to energy transfer between the 600 and 810 nm emission centers in the same particle. We used time-resolved fluorescence spectroscopy to study the luminescence lifetimes of the different types of GS-AuNPs at pH 7.5 (at this pH, the emissions of the dual-emissive NPs at 600 nm and 810 nm had the same intensities). Under 410 nm excitation, both the 600 nm- and 810 nm-emitting GS-AuNPs showed average luminescence lifetimes on the microsecond timescale: 1.54 μs for 600 nm emission and 1.93 μs for 810 nm emission (Figure 4A,B). However, in the case of the dual-emissive GS-AuNPs, we detected a nearly one-order decrease in the average lifetime of the 600 nm emission (0.14 μs) and a slight decrease in the average lifetime of the 810 nm emission to 1.20 μs. These results unambiguously indicate a strong energy transfer from a 600 nm emission center to a 810 nm emission center within the same dual-emissive ultrasmall AuNP (Figure 4C).

The energy transfer between these two emission centers is due to the overlap of the emission spectrum of the 600 nm emission center (donor) and the broad excitation spectrum of the 810 nm emission center (acceptor; Figure 1B,C). Interestingly, the energy transfer was sensitive to the pH value. As shown in Figure 3C, the donor emission (600 nm) dominated at pH 9, whereas the acceptor emission (810 nm) reached the highest value at pH 5. Not only the intensities but also the lifetimes of the dual emissions

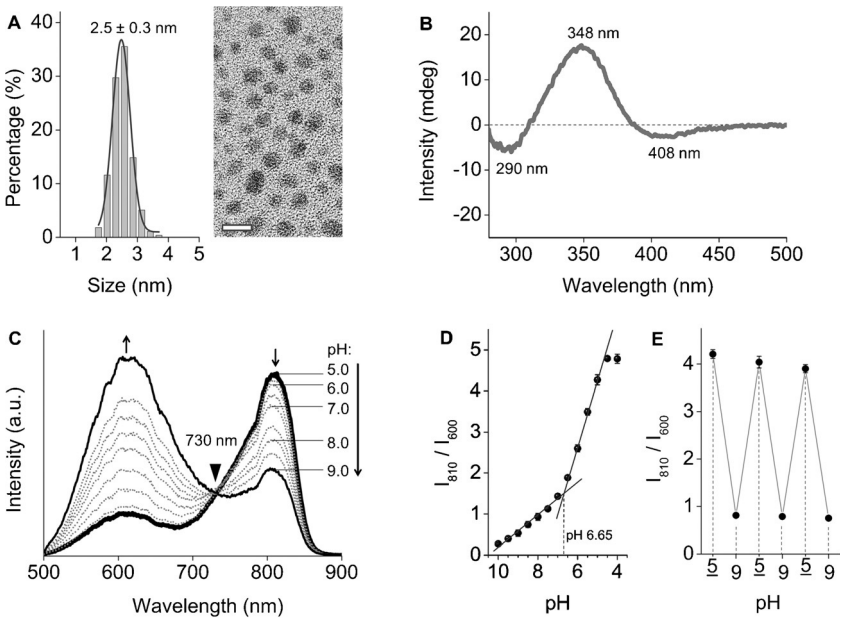

Figure 3. A) TEM image and core-size distribution of the dual-emissive GS-AuNPs. Scale bar: 5 nm. B) CD spectrum of the dual-emissive GS-AuNPs. C) Luminescence spectra of the dual-emissive GS-AuNPs in PBS buffer at different pH values. D) Ratiometric plot of the luminescence intensities at 600 nm and 810 nm over different pH values. E) Reversibility of the pH-dependent ratiometric emissions between pH 5.0 and pH 9.0.

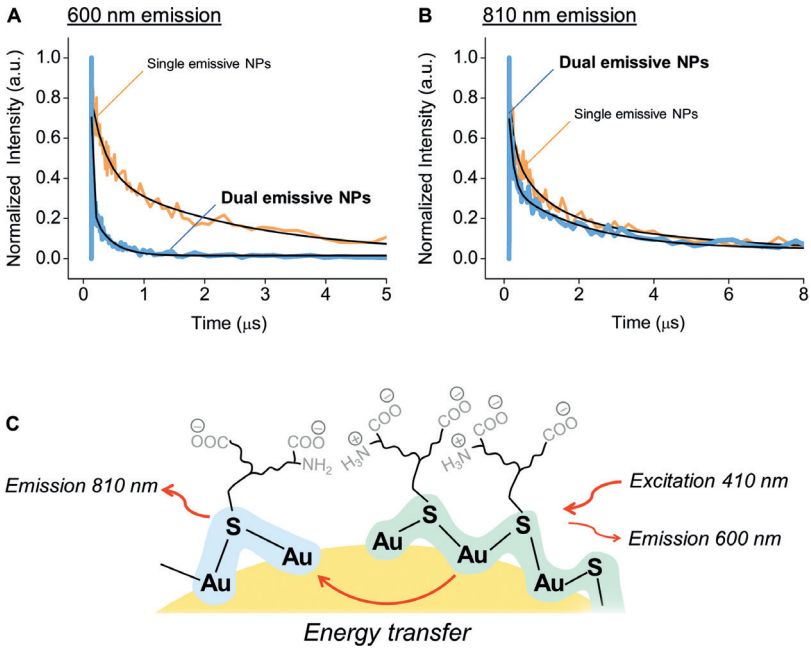

Figure 4. Luminescence lifetimes of the A) 600 nm emission and B) 810 nm emission of single-emissive GS-AuNPs (orange) and dual-emissive GS-AuNPs (blue) at pH 7.5. λ_{ex} = 410 nm for all measurements. C) Schematic representation of the energy transfer from a 600 nm emission center to a 810 nm emission center on one AuNP. Two amide bonds of glutathione are omitted for clarity.

were pH-dependent. Lowering the pH from 9 to 5 resulted in a decrease in the average lifetime of the 600 nm emission from 0.17 μs to 0.064 μs and an increase in the average lifetime of the 800 nm emission from 1.17 μs to 1.67 μs (Table S2). These results clearly indicate a significant enhancement of the energy transfer efficiency when the pH value is decreased from 9 to 5. As the energy-transfer efficiency is known to depend on the distance between the emission centers,[15] the observed increase in energy-transfer efficiency suggests the formation of more 600 nm emission centers on the particle surface, which was confirmed by EXAFS studies on the Au–S CNs of dual-emissive AuNPs. As shown in Table S3, the Au–S CN of dual-emissive NPs increased from 1.3 to 1.6 and 2.3 when the pH was decreased from 9 to 7 and 5. On the other hand, the CNs of the single-emissive AuNPs hardly responded to pH changes (Tables S4 and S5). Therefore, these changes in the Au–S and Au–N CNs of the dual-emissive AuNPs are likely due to the protonation of the amine group in acidic environments. At pH 5, the high degree of Au–S bonding suggests the formation of more 600 nm emission centers (donor), which might make energy transfer between the 600 nm and 800 nm emission centers more efficient. Thus, even though the 810 nm emission is pH-insensitive in single-emissive GS-AuNPs,[5b] it became highly pH-sensitive owing to stronger coupling with more 600 nm emission centers on the same NP.

In summary, with the assistance of CD, X-ray absorption, and optical spectroscopy, we unraveled the origin of the size-independent emission from ultrasmall GS-AuNPs with similar sizes but distinct emissions. The emission wavelengths strongly depended on the surface coverage and local binding structure of GSH on the AuNPs. A high surface coverage resulted in a high degree of Au–S bonding and strong Au^{I}→S charge transfer as well as 600 nm emission whereas a low surface coverage led to a low degree of Au–S bonding, relatively weak Au^{I}→ligand charge transfer, and 810 nm emission. The different CD responses of 600 nm- and 810 nm-emitting GS-AuNPs with the same size suggest that the CD signal strongly depends on the surface ligand coverage. Whereas the size-independent emissions suggest that surface coverage and local bonding environments play important roles in the emission from thiolated AuNPs, it should be noted that the gold core is important to stabilize the surface gold atoms and ligands. Moreover, based on previous studies on the long-lived NIR luminescence of Au_{25}, the d band of Au_{13} cores in Au_{25} is involved in the relaxation of excited electrons from Au–S charge transfer states to the ground states.[2b,16] Thus the d band of the Au cores of these luminescent AuNPs might also be involved in electron relaxation rather than excitation; however, more detailed ultrafast spectroscopy studies on these luminescent AuNPs are needed to fully understand their photoluminescence mechanism. Nevertheless, because the differently colored emissions were independent of the particle size but depended on the surface coverage, two differently colored emissions can be integrated into one single AuNP by tuning the ligand surface coverage. These dual-emissive AuNPs emitted in a unique pH-dependent ratiometric fashion owing to energy transfer between the two emission centers. This synergy not only offers an opportunity to modulate the photoluminescence of AuNPs but also provides a new approach to use luminescent AuNPs as ratiometric indicators for quantitative bioimaging.

Acknowledgements

This study was supported by the NIH (R01DK103363, CPRIT (RP140544), TexasMRC, and the start-up fund from the University of Texas at Dallas. P.N.D. is thankful for support through an NSERC CGS scholarship, and P.Z. acknowledges the NSERC DG grant.

Keywords: emission · gold · luminescence · nanoparticles · pH sensors

How to cite: *Angew. Chem. Int. Ed.* **2016**, *55*, 8894–8898
Angew. Chem. **2016**, *128*, 9040–9044

[1] a) J. Zheng, C. W. Zhang, R. M. Dickson, *Phys. Rev. Lett.* **2004**, *93*, 077402; b) J. Zheng, P. R. Nicovich, R. M. Dickson, *Annu. Rev. Phys. Chem.* **2007**, *58*, 409–431; c) J. Zheng, C. Zhou, M. Yu, J. Liu, *Nanoscale* **2012**, *4*, 4073–4083.

[2] a) G. Wang, T. Huang, R. W. Murray, L. Menard, R. G. Nuzzo, *J. Am. Chem. Soc.* **2005**, *127*, 812 – 813; b) M. S. Devadas, J. Kim, E. Sinn, D. Lee, T. Goodson, G. Ramakrishna, *J. Phys. Chem. C* **2010**, *114*, 22417 – 22423.
[3] a) J. Liu, M. Yu, C. Zhou, S. Yang, X. Ning, J. Zheng, *J. Am. Chem. Soc.* **2013**, *135*, 4978 – 4981; b) J. Liu, M. Yu, X. Ning, C. Zhou, S. Yang, J. Zheng, *Angew. Chem. Int. Ed.* **2013**, *52*, 12572 – 12576; *Angew. Chem.* **2013**, *125*, 12804 – 12808; c) J. Liu, M. Yu, C. Zhou, J. Zheng, *Mater. Today* **2013**, *16*, 477 – 486; d) J. Zhang, Y. Fu, C. V. Conroy, Z. Tang, G. Li, R. Y. Zhao, G. Wang, *J. Phys. Chem. C* **2012**, *116*, 26561 – 26569; e) M. Yu, J. Zheng, *ACS Nano* **2015**, *9*, 6655 – 6674.
[4] a) M. Yu, J. Liu, X. Ning, J. Zheng, *Angew. Chem. Int. Ed.* **2015**, *54*, 15434 – 15438; *Angew. Chem.* **2015**, *127*, 15654 – 15658; b) M. Yu, J. Zhou, B. Du, X. Ning, C. Authement, L. Gandee, P. Kapur, J.-T. Hsieh, J. Zheng, *Angew. Chem. Int. Ed.* **2016**, *55*, 2787 – 2791; *Angew. Chem.* **2016**, *128*, 2837 – 2841.
[5] a) C.-C. Huang, Z. Yang, K.-H. Lee, H.-T. Chang, *Angew. Chem. Int. Ed.* **2007**, *46*, 6824 – 6828; *Angew. Chem.* **2007**, *119*, 6948 – 6952; b) S. Sun, X. Ning, G. Zhang, Y.-C. Wang, C. Peng, J. Zheng, *Angew. Chem. Int. Ed.* **2016**, *55*, 2421 – 2424; *Angew. Chem.* **2016**, *128*, 2467 – 2470.
[6] a) C. Zhou, C. Sun, M. Yu, Y. Qin, J. Wang, M. Kim, J. Zheng, *J. Phys. Chem. C* **2010**, *114*, 7727 – 7732; b) M. Yu, C. Zhou, J. Liu, J. D. Hankins, J. Zheng, *J. Am. Chem. Soc.* **2011**, *133*, 11014 – 11017.
[7] a) X. J. Tu, W. B. Chen, X. Q. Guo, *Nanotechnology* **2011**, *22*, 095701; b) C. Zhou, G. Y. Hao, P. Thomas, J. B. Liu, M. X. Yu, S. S. Sun, O. K. Oz, X. K. Sun, J. Zheng, *Angew. Chem. Int. Ed.* **2012**, *51*, 10118 – 10122; *Angew. Chem.* **2012**, *124*, 10265 – 10269.
[8] Z. Luo, X. Yuan, Y. Yu, Q. Zhang, D. T. Leong, J. Y. Lee, J. Xie, *J. Am. Chem. Soc.* **2012**, *134*, 16662 – 16670.
[9] a) T. Huang, R. W. Murray, *J. Phys. Chem. B* **2001**, *105*, 12498 – 12502; b) S. E. Crawford, C. M. Andolina, A. M. Smith, L. E. Marbella, K. A. Johnston, P. J. Straney, M. J. Hartmann, J. E. Millstone, *J. Am. Chem. Soc.* **2015**, *137*, 14423 – 14429.
[10] P.-C. Chen, T.-Y. Yeh, C.-M. Ou, C.-C. Shih, H.-T. Chang, *Nanoscale* **2013**, *5*, 4691 – 4695.
[11] a) T. G. Schaaff, R. L. Whetten, *J. Phys. Chem. B* **2000**, *104*, 2630 – 2641; b) Z. Wu, C. Gayathri, R. R. Gil, R. Jin, *J. Am. Chem. Soc.* **2009**, *131*, 6535 – 6542.
[12] a) H. Yao, T. Fukui, K. Kimura, *J. Phys. Chem. C* **2008**, *112*, 16281 – 16285; b) C. Gautier, T. Bürgi, *J. Am. Chem. Soc.* **2008**, *130*, 7077 – 7084; c) C. Zeng, T. Li, A. Das, N. L. Rosi, R. Jin, *J. Am. Chem. Soc.* **2013**, *135*, 10011 – 10013; d) I. Dolamic, B. Varnholt, T. Burgi, *Nat. Commun.* **2015**, *6*, 7117.
[13] a) H. Qian, W. T. Eckenhoff, Y. Zhu, T. Pintauer, R. Jin, *J. Am. Chem. Soc.* **2010**, *132*, 8280 – 8281; b) P. D. Jadzinsky, G. Calero, C. J. Ackerson, D. A. Bushnell, R. D. Kornberg, *Science* **2007**, *318*, 430 – 433.
[14] P. Zhang, *J. Phys. Chem. C* **2014**, *118*, 25291 – 25299.
[15] J. R. Lakowicz, *Principles of Fluorescence Spectroscopy*, *3rd ed.*, Springer, New York, **2006**, p. 13.
[16] M. Zhu, C. M. Aikens, F. J. Hollander, G. C. Schatz, R. Jin, *J. Am. Chem. Soc.* **2008**, *130*, 5883 – 5885.

Received: March 20, 2016
Revised: April 29, 2016
Published online: June 27, 2016

